Role of Disulfide Bonds in the Stability of Recombinant Manganese Peroxidase†

N. Scott Reading and Steven D. Aust*

Biotechnology Center, Department of Chemistry and Biochemistry, Utah State University, Logan, Utah 84322-4705

Received March 5, 2001; Revised Manuscript Received April 13, 2001

ABSTRACT: *Phanerochaete chrysosporium* manganese peroxidase (MnP) [isoenzyme H4] was engineered with additional disulfide bonds to provide structural reinforcement to the proximal and distal calcium-binding sites. This rational protein engineering investigated the effects of multiple disulfide bonds on the stabilization of the enzyme heme environment and oxidase activity. Stabilization of the heme environment was monitored by UV−visible spectroscopy based on the electronic state of the alkaline transition species of ferric and ferrous enzyme. The optical spectral data confirm an alkaline transition to hexacoordinate, low-spin heme species for native and wild-type MnP and show that the location of the engineered disulfide bonds in the protein can have significant effects on the electronic state of the enzyme. The addition of a single disulfide bond in the distal region of MnP resulted in an enzyme that maintained a pentacoordinate, high-spin heme at pH 9.0, whereas MnP with multiple engineered disulfide bonds did not exhibit an increase in stability of the pentacoordinate, high-spin state of the enzyme at alkaline pH. The mutant enzymes were assessed for increased stability by incubation at high pH. In comparison to wild-type MnP, enzymes containing engineered disulfide bonds in the distal and proximal regions of the protein retained greater levels of activity when restored to physiological pH. Additionally, when assayed for oxidase activity at pH 9.0, proteins containing engineered disulfide bonds exhibited slower rates of inactivation than wild-type MnP.

Phanerochaete chrysosporium, a ubiquitous and perhaps archetypal white-rot fungus, is capable of degrading lignin and a wide variety of environmental pollutants (*1*) by secreting lignin (LiP)[1] and manganese peroxidases (MnP) as part of an extracellular degradation system produced during secondary metabolism (*2*, *3*). These peroxidases belong to the class II (secreted fungal peroxidases) of the plant peroxidase superfamily (*4*) and share a high degree of sequence and structural similarity (*5*, *6*). The enzymes also follow a classical peroxidase catalytic cycle (*4*), have low pH optima for the oxidation of their respective substrates (*4*), and produce oxidized products with high redox potentials (*7*, *8*). Lignin peroxidase can oxidize a wide variety of substrates. Manganese peroxidase is unique in its ability to oxidize Mn^{2+} to Mn^{3+}, which acts as a diffusible oxidant contributing to the biodegradative potential of the fungus (*9*, *10*).

The crystal structure of MnP has been solved (*5*). The protein's structure has the same basic fold as the class III plant peroxidase, peanut peroxidase (PNP) (*11*), with the heme prosthetic group sandwiched between the B and F helices. The F helix contributes a histidine residue as the fifth ligand to the heme iron, while the B helix provides two residues (His, Arg) that are involved in the reaction of hydrogen peroxide with the heme iron (*5*). Other structural similarities are two calcium-binding sites, proximal and distal to the heme, and a high number of disulfide bridges within the protein (*5*, *11*). Manganese peroxidase contains five disulfide bridges (Cys3−Cys15, Cys14−Cys289, Cys33−Cys117, Cys253−Cys319, and Cys341−Cys348), one more than PNP, but two of which are in analogous positions in PNP (*5*, *11*). The uniquely positioned disulfide bonds in MnP are located near the N-terminus of the B helix and C-terminus of D helix (Cys33−Cys117), and within the C-terminus, random coil structure of the protein (Cys253−Cys319, Cys341−Cys348) (*5*).

Several studies have been carried out to understand the structural stability of MnP. Glycosylation of the native peroxidases was shown to have a role in stabilizing the protein against inactivation (*12*). Recombinant MnP was observed to inactivate at a faster rate than native MnP, a trait that was attributed to the lack of glycosylation on the recombinant enzyme. Calcium appears to have a critical role in stabilizing MnP against inactivation. Inactivation of native MnP was correlated with the loss of at least one calcium from the protein (*13*, *14*). The calcium was proposed to be the released from the distal calcium-binding site, resulting in the formation of a sixth ligand to the heme iron by a distal histidine leading to inactivation (*15*). Recent publications have provided evidence supporting the proposition that fungal peroxidases form a bis(histidyl) heme complex when exposed to conditions that lead to inactivation (*16*, *17*). In each of these studies, the addition of exogenous calcium resulted in a restoration of enzyme activity. However, Sutherland et al.

† This research was supported by Stockhausen GmbH & Co., KG, PO Box 570, D-47705, Krefeld, Germany.

* To whom correspondence should be addressed at 211 Biotechnology Center, Department of Chemistry and Biochemistry, Utah State University, Logan, UT 84322-4705. Telephone (435) 797-2730; Fax (435) 797-2755; email: sdaust@cc.usu.edu.

[1] Abbreviations: MnP, manganese peroxidase; LiP, lignin peroxidase; PNP, peanut peroxidase; TRIS, tris(hydroxymethyl)aminomethane; LMCT, ligand-to-metal charge transfer; ESR, electron spin resonance spectroscopy.

10.1021/bi010440i CCC: $20.00
Published on Web 06/14/2001

Table 1: Primers for Site-Directed Mutagenesis of *mnp* DNA[a]

primer ID	forward primer (5′−3′)	restriction site
mnp C33A	GTTCCAGGGTGA**CGC**CGGCGAAGATGCCCAC	*Hin*1I
mnp A48C	GTCTGACCTTCCACGAC**TGC**ATTGCAATCTCCCAG	*Bse*MI
mnp S52C	CGACGCTATTGC**C**AT**A**T**G**CCGGAGCCTAGG	*Nde*I
mnp A59C	CCTAGGTCC**A**CAG**TG**TGGCGGCGGTGC	*Ade*I
mnp A63C	GGCTGGCCGGCGGA**TG**TGACGGCTCCATGC	*Tsp*45I
mnp T174C	CTCCTGGCTTCACAC**TGT**GTTGCTCGTGCGGAC	*Ade*I
mnp D182C	CGGACAAGGTC**TG**CGAGACCATCGATGC	*SalI*[b]
mnp V201C	ACCTTCGACACCCAG**TGC**TTCCTCGAGGTCCTG	*Ade*I
mnp G214C	CAGGCTTCCCG**T**GCTCGAACAACAACACCG	*Alw*21I

[a] Target codons are underlined and sequence changes bolded. [b] Represents a deletion of a restriction site in the mutated sequence.

demonstrated that the extent of recovery of activity was inversely dependent upon the duration of exposure to extreme conditions, suggesting that other structural rearrangements were occurring within the protein causing the enzyme to conform to an irreversibly inactivated state (*13*). These observations suggested that protein structure could possibly be reinforced using disulfide bonds, thereby preventing the protein from adopting an irreversible, inactivated state after prolonged exposure to extreme conditions. This work was initially accomplished and shown to be successful with the addition of a disulfide bond near the distal calcium-binding site (*18*). This paper addresses the effect of various engineered disulfide bonds on the stability and activity of MnP.

EXPERIMENTAL PROCEDURES

Chemicals. Oxidized and reduced glutathione were purchased from Boehringer Mannheim (Indianapolis, IN). Reagents used in polymerase chain reaction were purchased from Stratagene (LaJolla, CA). GeneRuler 100 basepair DNA Ladder Plus and restriction enzymes *Sal*I, *Alw*21I, *Hin*1I, *Ade*I, *Bse*MI, and *Nde*I were purchased from MBI Fermentas (Amherst, NY). Restriction enzyme *Tsp*45I was purchased from New England Biolabs (Beverly, MA). Nusieve 3:1 Agarose was purchased from FMC Bioproducts (Rockland, ME). All other chemicals were purchased from Sigma Chemical Co. (St. Louis, MO). Hydrogen peroxide concentrations were quantified using $\epsilon_{240} = 39.4\ M^{-1}\ cm^{-1}$ (*19*). All aqueous solutions were prepared using purified water (Barnsted NANOpure II system; specific resistance 17.0 $M\Omega \cdot cm^{-1}$). All chemicals were of the highest grade available.

Site-Directed Mutagenesis. Site-directed mutagenesis was conducted as previously described (*18*). Macromolecular Resources (Department of Biochemistry, Colorado State University, Fort Collins, CO) synthesized the primers for site-directed mutagenesis (Table 1).

Production of Manganese Peroxidase. Manganese peroxidase [isoenzyme H4] was purified from liquid cultures of *P. chrysosporium* as previously described (*20*). The enzyme concentration was determined using the $\epsilon_{406} = 127\ mM^{-1}\ cm^{-1}$ (*21*). The preparation and purification of recombinant MnP was as previously described (*18*). The purified recombinant enzymes had RZ values (A_{406}/A_{280}) of 3 or greater. Formation of disulfide bonds was verified by assaying for sulfhydryl groups using the Thiol and Sulfide Quantitation kit from Molecular Probes, Inc. (Eugene, OR).

UV−Visible Spectroscopy and Enzyme Stability Studies. Spectral properties of ferric and ferrous MnP were recorded using a Shimadzu UV-2101PC spectrophotometer (Columbia, MD). Samples were prepared by combining enzyme (~3 μM final concentration) with 50 mM acetate buffer, pH 5.0, or 50 mM borate buffer, pH 9.0, in a 0.5-mL quartz cuvette. The enzymes were reduced by the addition of excess dithionite. The samples were allowed to equilibrate after the addition of secondary components, such as dithionite, calcium, imidazole, or buffers, prior to the spectra being recorded. Investigations of enzyme stability were conducted as previously described (*18*). The oxidation of Mn^{2+} was measured by following the formation of Mn^{3+}-oxalate complex using $\epsilon_{270} = 5500\ M^{-1}\ cm^{-1}$ (*22*). Hanker−Yates reagent (*23*), prepared just prior to use by combining catechol and *p*-phenylenediamine in a 2:1 molar ratio, was added to a cuvette containing 50 mM borate buffer, pH 9.0, and 0.1 mM hydrogen peroxide. Oxidation assays were initiated by the addition of enzyme (final concentration 30 nM) to the reaction cuvette. The extinction coefficient of the product of Hanker−Yates reagent oxidation was determined at pH 9.0 by the complete reaction of limiting hydrogen peroxide with MnP and excess substrate in the presence of 1 mM calcium. All data points represent the average from at least three assays. The data were fit to an exponential decay function and apparent inactivation rates determined.

Electron Spin Resonance Spectroscopy. The electron spin resonance (ESR) spectrum was recorded on a Bruker ECS-106 spectrometer (Bruker Instruments, Billerica, MA), operating at 9.8 GHz and 50 kHz modulation frequency. The sample was prepared by reacting 30 nM MnP with 1 mM *p*-phenylenediamine and hydrogen peroxide in borate buffer, pH 9.0, in a 0.5-mL quartz cuvette at 25 °C. Production of the radical was monitored at 462 nm on a Shimadzu UV-2101PC spectrophotometer prior to the sample being loaded into a quartz flat cell for measurement.

RESULTS

Site-Directed Mutagenesis of Manganese Peroxidase. Engineering disulfide bonds into MnP was achieved through site-directed mutagenesis of the *mnp* gene using the primer sets listed in Table 1 and as described in Experimental Procedures. The location of the modified amino acids within MnP structure are illustrated in Figure 1 and a summary of the disulfide bond variants used in this study are listed in Table 2. The introduction of a sixth disulfide bond was attempted near the distal calcium-binding site at two different locations. On the basis of molecular modeling, cysteine residues were introduced within the 14 amino acid random coil loop that extends between the B and B′ helices replacing amino acids Ser52 and Ala59 (S52C/A59C). Separately, based on homology modeling using peanut peroxidase (PNP)

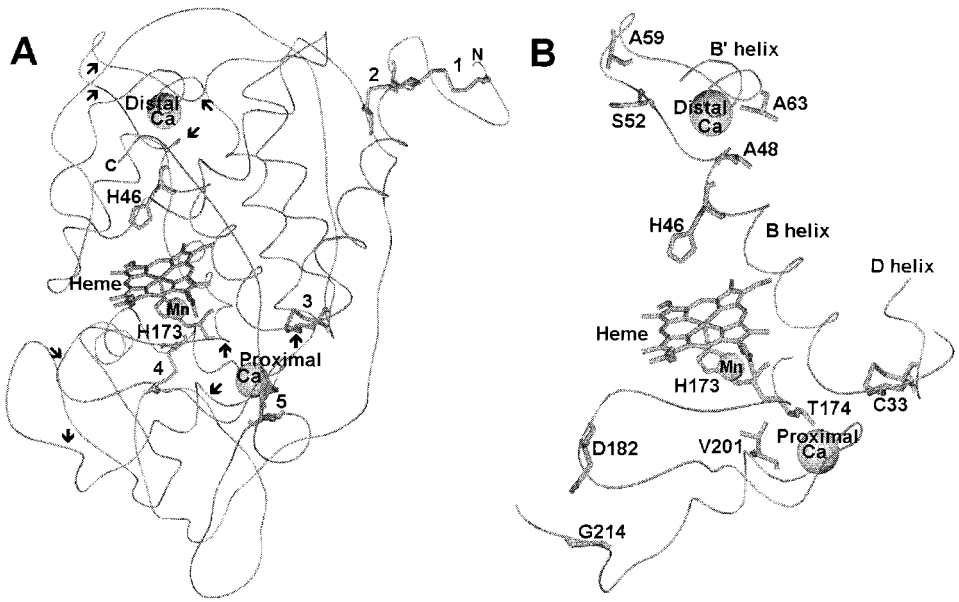

FIGURE 1: Ribbon diagram depicting the structure of manganese peroxidase from *P. chrysosporium* (*5*). (A) The naturally occurring disulfide bonds (bond number shown in brackets, [1] Cys3-Cys15, [2] Cys14-Cys289, [3] Cys33-Cys117, [4] Cys253-Cys319, [5] Cys341-Cys348) are shown in relation to the heme, manganese ion, distal (H46) and proximal (H173) histidines, and distal and proximal calcium ions. Arrows within MnP structure indicate the location of the amino acids that were modified. N and C indicate the amino and carboxy termini of the protein, respectively. (B) Detailed view of MnP structure showing the location and arrangement of the amino acids that were modified in relation to major structural elements in MnP.

Table 2: Description of Disulfide Bond Variants of Manganese Peroxidase

	disulfide bond content			
manganese peroxidase	total	added	deleted	location of modification
native MnP	5			
wild-type MnP	5			
C33A	4		1	N-terminus of B helix
S52C/A59C	6	1		distal region
A48C/A63C	6	1		distal region
C33A/A48C/A63C	5	1	1	distal region and N-terminus of B helix
A48C/A63C/T174C/V201C	7	2		distal and proximal region
A48C/A63C/D182C/G214C	7	2		distal and proximal region

Table 3: Spectral Features of Disulfide Bond Variant Manganese Peroxidases

manganese peroxidase	Soret	visible region bands		
native MnP	407	503	538(sh)	636
wild-type MnP	407	502	538(sh)	636
C33A	406	502	538(sh)	638
S52C/A59C	403			
A48C/A63C	406	504	542(sh)	640
C33A/A48C/A63C	406	502	537(sh)	638
A48C/A63C/T174C/V201C	395			
A48C/A63C/D182C/G214C	407	504	542(sh)	640

structure, cysteine residues were introduced at positions Ala48 and Ala63 (A48C/A63C) in MnP, adjacent to the distal calcium-binding site (*18*). These two disulfide bonds variants would each have formed a protein with the B-helix anchored at both the N-terminus and C-terminus by disulfide bonds. Amino acid residue Cys33 at the N-terminus of the B-helix was mutated to an alanine (C33A/A48C/A63C) to determine if the C-terminus disulfide bond (A48C−A63C) was sufficient to stabilize MnP. The Cys33 codon was also mutated in wild-type *mnp* DNA sequence to create the C33A mutant protein. Additive to the six-disulfide bond A48C/A63C variant, cysteine codons were introduced into the *A48C/A63C mnp* DNA to generate an enzyme with seven disulfide bonds. The introduction of the seventh disulfide bond was attempted at two locations. The first site chosen was adjacent to the MnP proximal calcium-binding site at amino acids Thr174 and Val201 (A48C/A63C/T174C/V201C). The second site chosen was based on the PNP structural model to introduce a disulfide bond at amino acids Asp182 and Gly214 (A48C/A63C/D182C/G214C) between the proximal histidine ligand and the proximal calcium-binding site. All disulfide bond variants of MnP were expressed in *Escherichia coli* and during folding were constituted with heme and calcium.

UV−Visible Spectroscopy of Manganese Peroxidase Disulfide Bond Variants. The purified disulfide bond variants C33A, C33A/A48C/A63C, A48C/A63C, and A48C/A63C/D182C/G214C had spectral features similar to wild-type, ferric MnP. The spectral features, listed in Table 3, show the Soret maximum centered at 406/407 nm and ligand-to-metal charge-transfer bands (LMCT) near 500 and 637 nm, indicative of a pentacoordinate, high-spin heme iron. The spectral properties of the S52C/A59C and A48C/A63C/T174C/V201C mutants differed from that of wild-type ferric MnP with Soret maxima centered at 403 and 395 nm, respectively, and the enzymes were not active.

The spectral properties of the MnP disulfide bond variants were compared to native and wild-type MnP under acidic (pH 5.0) and alkaline (pH 9.0) conditions. At pH 5.0, the enzymes exhibited absorption spectra indicative of pentacoordinate, high-spin heme proteins. At pH 9.0 (50 mM borate buffer), the spectra observed for native and wild-type ferric MnP indicated that the enzymes had adopted a hexacoordinate, low-spin state (Figure 2, Table 4).[2] Soret absorption decreased in intensity and a shoulder at 360 nm

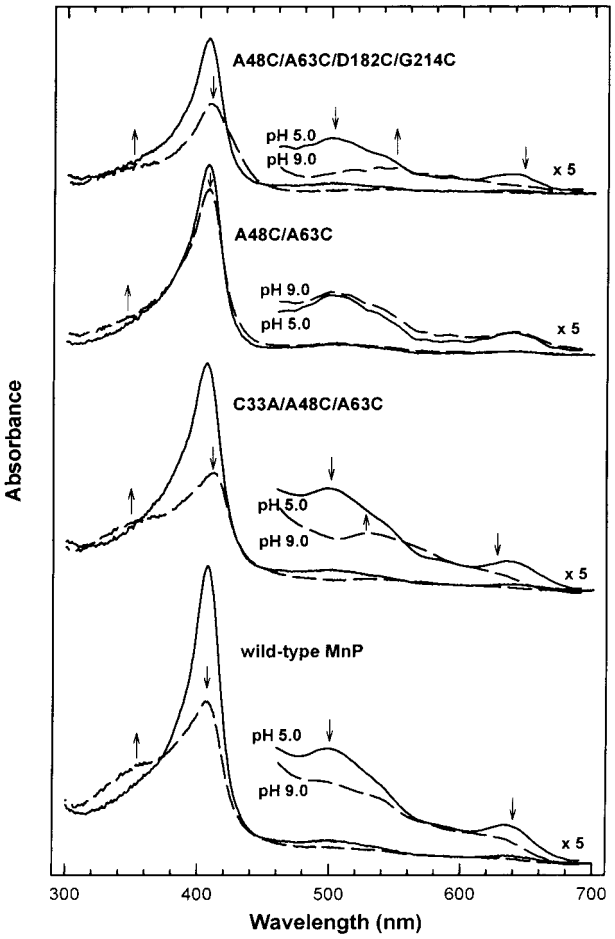

FIGURE 2: Electronic absorption spectra of oxidized (ferric) wild-type MnP, C33A/A48C/A63C, A48C/A63C, and A48C/A63C/D182C/G214C. The spectra were obtained in 50 mM acetate buffer, pH 5.0 (−) and in 50 mM borate buffer, pH 9.0 (- - -). Arrows indicate the direction of major changes in the absorption spectra. Details of the experimental conditions are described in Experimental Procedures.

appeared. The visible bands at 505 and 637 nm disappeared and were replaced by a broad absorption across the 500 nm region with an apex at 535 nm. The spectral changes observed for alkali-treated, ferric C33A, C33A/A48C/A63C, and A48C/A63C/D182C/G214C were similar to the spectral properties of alkali-treated, ferric native and wild-type MnP. However, alkali-treated, ferric A48C/A63C spectral features indicated that the enzyme did not undergo an alkaline transition to a hexacoordinate, low-spin state but retained a pentacoordinate, high-spin heme (Figure 2). The spectrum of A48C/A63C (recorded within the first minute of exposure to alkaline conditions) showed a 20% decrease in Soret absorbance and a 40% decrease in LMCT absorbance (Figure 3). Absorption maximum red-shifted in the Soret region to 408 nm and in the LMCT region from 503 to 510 nm. The absorption maximum at 636 nm was not altered. In a second spectrum (recorded within the second minute after exposure to alkaline conditions), LMCT absorbance had increased, returning to levels equivalent to 80% of the original absorption values in the 500 and 600 nm regions. Absorption

[2] The spectral data for native MnP was not included because it was published previously (*16*). The spectral data for C33A mutant MnP was not included because it was essentially identical to the spectra recorded for C33A/A48C/A63C mutant MnP.

Table 4: Spectral Features of Oxidized and Reduced Manganese Peroxidase at pH 5.0 and 9.0

manganese peroxidase	pH	electronic absorption maximum (nm)				
ferric native MnP	5.0		407	505	535(sh)	637
	9.0	360(sh)	407		535	
ferric wild-type MnP	5.0		407	501	535(sh)	637
	9.0	360(sh)	407		535	
ferric C33A	5.0		407	504	538(sh)	638
	9.0	360(sh)	409		535	
ferric A48C/A63C	5.0		407	505	532(sh)	640
	9.0		407	505	535(sh)	640
ferric C33A/A48C/A63C	5.0		407	504	537(sh)	640
	9.0	360(sh)	409		535	
ferric A48C/A63C/ D182C/G214C	5.0		406	501	535(sh)	638
	9.0	360(sh)	407		532	
ferrous native MnP	5.0		436		556	588
	9.0		425	529	559	
ferrous wild-type MnP	5.0		437		558	589
	9.0		423	530	559	
ferrous C33A	5.0		436		556	589
	9.0		424	526	559	
ferrous A48C/A63C	5.0		436		556	587
	9.0		438		558	590
ferrous C33A/A48C/A63C	5.0		436		556	589
	9.0		424	526	559	
ferrous A48C/A63C/ D182C/G214C	5.0		435		557	589
	9.0		438		557	589

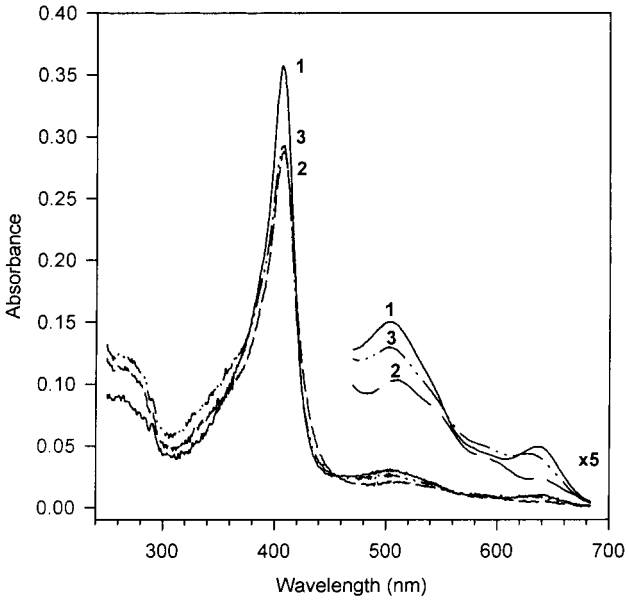

FIGURE 3: Changes in the electronic absorption spectra of A48C/A63C during exposure to alkaline pH. Spectra were recorded [1] prior to the addition of borate buffer, pH 9.0, [2] at 30 s following the addition of the borate buffer, and [3] at 2 min after the addition of the borate buffer to the protein. Each scan took approximately 45 s to record. Spectra recorded at 15, 30, 45, and 60 min following the addition of borate buffer were virtually identical to spectrum 3. Details of the experimental conditions are described in Experimental Procedures.

maximum at 510 nm was blue-shifted to 504 nm and the 636 nm peak blue-shifted to 630 nm. Soret absorption increased slightly and blue-shifted to 407 nm (Figure 3). The resulting absorption spectrum of A48C/A63C remained unchanged for at least an hour.

The ferric heme iron of MnP was reduced to ferrous iron using dithionite and the spectra of each enzyme was recorded at acidic and alkaline pH (Figure 4 and Table 4).[2] The

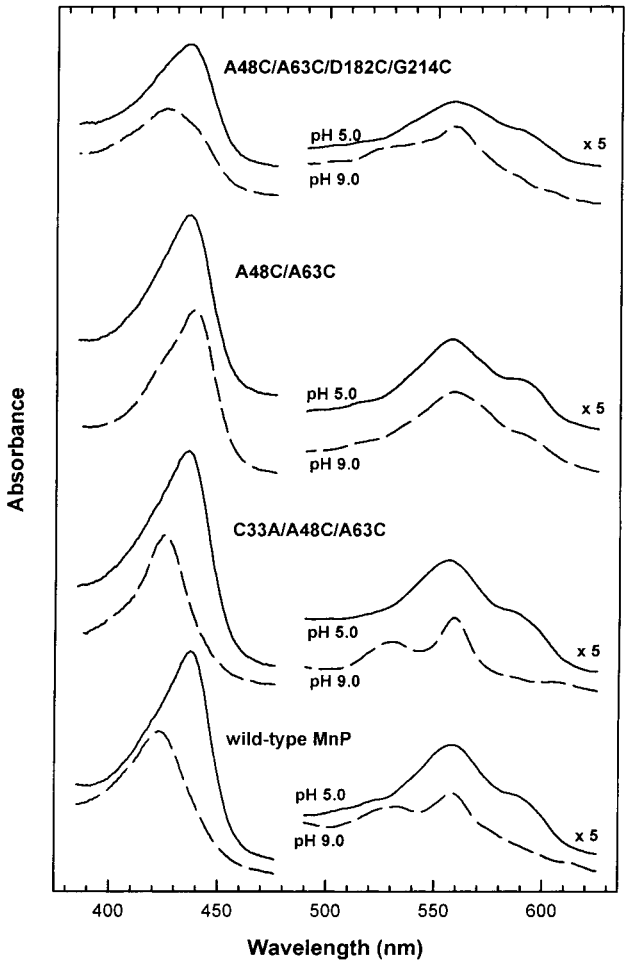

FIGURE 4: Electronic absorption spectra of reduced (ferrous) wild-type MnP, C33A/A48C/A63C, A48C/A63C, and A48C/A63C/D182C/G214C. The spectra were obtained in 50 mM acetate buffer, pH 5.0 (−) and in 50 mM borate buffer, pH 9.0 (- - -). Details of the experimental conditions are described in Experimental Procedures.

spectral characteristics of ferrous native and wild-type MnP at pH 5.0 and 9.0 were consistent with previously published data (*16*). At acidic pH, the Soret absorbance was red-shifted to 436 nm and absorbance maxima at 556 and 588 nm appeared. At alkaline pH, the Soret absorbance decreased and blue-shifted to 425−423 nm and absorbance at 529 nm appeared, while absorbance at 556 nm red-shifted to 559 nm and absorbance at 588 nm disappeared. The spectral features of ferrous C33A, A48C/A63C, C33A/A48C/A63C, and A48C/A63C/D182C/G214C at pH 5.0 were similar to those reported for native and wild-type MnP, with absorption peaks at 436, 556, and 590 nm. Additionally, the absorption spectra of ferrous C33A, C33A/A48C/A63C, and A48C/A63C/D182C/G214C at alkaline pH were similar to that observed for wild-type MnP. However, the spectrum of ferrous A48C/A63C at alkaline pH remained centered at 436, 556, and 590 nm, indicative of a pentacoordinate, high-spin state (Figure 4, Table 4).

Effect of Calcium on Alkali-Treated Manganese Peroxidase. The alkali-treated, ferric enzymes, except C33A and C33A/A48C/A63C, responded to exogenous calcium (1 mM $CaCl_2$) consistent with previously published reports (*16*). Soret and LMCT absorption bands were restored to their original intensities (adjusted for dilution effects) at 407, 503, and 635 nm, indicative of pentacoordinate, high-spin heme. The adjustment of buffer pH to 5.0 following the addition of calcium caused a sharpening of the spectral features of the MnP variants but did not alter the absorption maxima of the major absorbance peaks. With the exception of MnPA48C/A63C, if the pH was adjusted to 5.0 prior to the addition of exogenous calcium, the Soret absorption was dramatically decreased and the enzymes were not active. The addition of calcium to alkali-treated, ferric C33A and C33A/A48C/A63C caused a loss of Soret absorbance, which was replaced with absorbance at 390 nm and a loss of absorption bands in the visible region due aggregation of the protein in the cuvette.

Effect of Disulfide Bonds on the Stabilization of Manganese Peroxidase Activity. The effects of temperature and pH on the stability of native MnP, wild-type MnP and A48C/A63C were shown previously (*18*). The disulfide bond variants C33A, C33A/A48C/A63C, and A48C/A63C/D182C/G214C were assayed for Mn^{2+} oxidase activity after incubation at 37 °C at various pH (Figure 5). In comparison to A48C/A63C, A48C/A63C/D182C/G214C retained greater activity at pH 7.0 and pH 8.0. At pH 8.0, the seven-disulfide bond MnP variant retained ∼50% of its original activity. The MnP variants with the C33A mutation were considerably less stable, inactivating at pH 7.0 in a time period comparable to that of wild-type enzyme.

Enzyme activity was also assayed at pH 9.0 to determine whether functionality correlated with the spectroscopic data. The pH-dependent Mn^{2+} oxidation profiles for native, wild-type, and mutant MnP were compared (data not shown). Each of the enzymes were equally inefficient at oxidizing Mn^{2+} at pH greater than 6.5. Therefore, it was necessary to find an alternative reductant to assess enzymatic activity at pH 9.0. The reductant chosen was *p*-phenylenediamine. This was combined with catechol, which reacts with oxidized *p*-phenylenediamine to form a darkly colored product that has maximal absorbance at 525 nm and an estimated extinction coefficient of 4000 M^{-1} cm^{-1} at pH 9.0. The two reagents, when used together, are known as Hanker−Yates reagent, which has been used as an indicator of peroxidase activity for many years (*23*). The reaction of MnP with Hanker−Yates reagent is independent of the presence of Mn^{2+} and results in turnover of the enzyme across a broad pH range, maximal at pH 6.5. Although each component of Hanker−Yates reagent is a reductant for MnP, it was determined that catechol was not oxidized by MnP at pH 9.0. However, *p*-phenylenediamine was oxidized by MnP at pH 9.0 and formed the one-electron oxidized radical (A_{max} 460 nm) which was confirmed by ESR (*24*) (Figure 6A, inset).

Wild-type MnP was most susceptible to the effects of pH, exhibiting a slower initial rate of Hanker−Yates reagent oxidation (∼8 s^{-1}) and rapid inactivation (within ∼75 s) at pH 9.0 than the other enzymes (Figure 6A). The initial oxidation rates for native MnP, A48C/A63C, and A48C/A63C/D182C/G214C were 11, 17, and 14 s^{-1}, respectively, but the duration of oxidation differed for these enzymes (>200, >300, and ∼150 s, respectively). A graph of the oxidation rates (taken at 5-s intervals) for these four enzymes illustrate the change in the rates of oxidation over the first 300 s of the reaction (Figure 6B). The initial rate of inactivation for native MnP was 0.1 s^{-1}, determined as the decrease in the rate of Hanker−Yates reagent oxidation, whereas the initial inactivation rates for wild-type MnP,

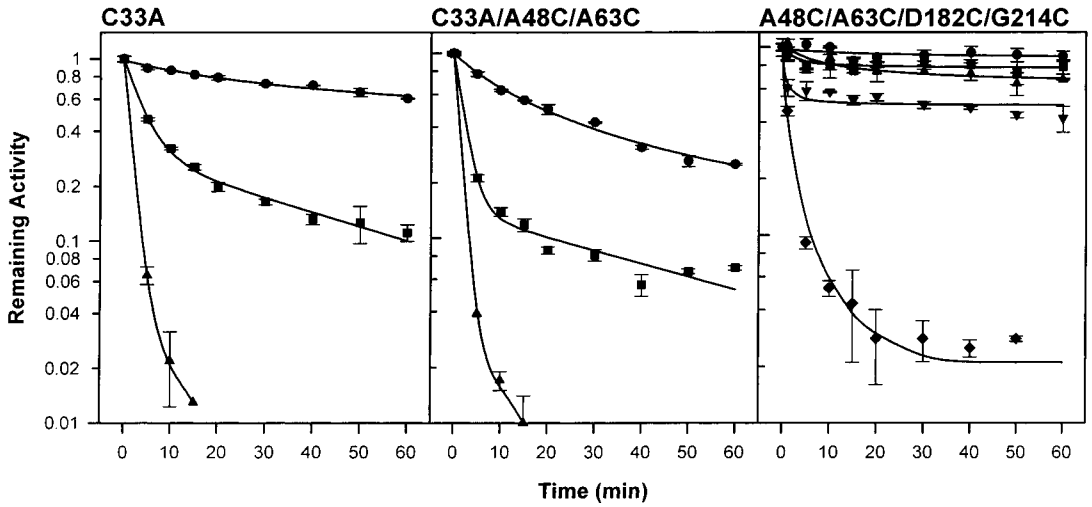

FIGURE 5: Effect of pH on the inactivation of C33A, C33A/A48C/A63C, and A48C/A63C/D182C/G214C. The enzymes were incubated at 37 °C in 20 mM acetate buffer, pH 4.5 (●), 20 mM acetate buffer, pH 6.0 (■), and 20 mM tris(hydroxymethyl)aminomethane (TRIS)-HCl, pH 7.0 (▲). A48C/A63C/D182C/G214C was additionally incubated in 20 mM TRIS-HCl, pH 8.0 (▼) and 20 mM borate buffer, pH 9.0 (◆). Assay conditions were 30 nM enzyme, 0.4 mM Mn^{2+}, 100 mM acetate buffer (pH 4.5), 1 mM oxalate, 0.1 mM H_2O_2.

A48C/A63C, and A48C/A63C/D182C/G214C were 0.2 s^{-1}. When the oxidation rates were plotted on a logarithmic scale, the rate of inactivation for native MnP, wild-type MnP, and A48C/A63C/D182C/G214C were found to be linear (Figure 6B, inset). However, the rate of inactivation of A48C/A63C changed from 0.2 to 0.02 s^{-1} at about 50 s and this slower rate of inactivation continued through the remaining time of the assay.

Exogenous calcium increased the rate and duration that MnP was able to oxidize Hanker−Yates reagent at pH 9.0 (Figure 7A). Although similar amounts of each enzyme were used in these experiments, wild-type MnP did not exhibit the same rates of oxidation as native MnP, A48C/A63C, and A48C/A63C/D182C/G214C when calcium (1 mM) was present in the assay mixture. Upon addition of calcium, the enzymes underwent a reactivation phase followed by a slow inactivation phase (Figure 7B). The rates of inactivation for native MnP (0.05 s^{-1}), wild-type MnP (0.03 s^{-1}), A48C/A63C (0.05 s^{-1}), and A48C/A63C/D182C/G214C (0.04 s^{-1}) in the presence of additional calcium were linear and about 10-fold slower than the inactivation rates observed previously for the enzymes.

DISCUSSION

Six variants of MnP were produced that contained combinations of engineered disulfide bonds near the calcium-binding sites. Four of the six variants were active and had characteristic absorption spectra of pentacoordinate, high-spin, ferric MnP, indicating that the modifications introduced into the protein did not adversely affect the liganding environment of the heme iron. However, two MnP variants containing disulfide bonds introduced at positions Ser52 and Ala59, and Thr174 and Val201 in combination with A48C and A63C appeared to have disturbed the heme environment such that the Soret bands were shifted from 406 nm and the proteins were not active.

The coordination state of ferric and ferrous MnP has been correlated to electronic absorption spectral features of MnP by resonance Raman spectroscopy (*16*). Our data for native and wild-type MnP agree with the reported spectral features of the alkaline transition state for the fungal peroxidases (*16*, *17*). The electronic absorption spectra of the disulfide bond MnP variants were similarly analyzed at acidic and alkaline pH. The optical spectra of the two C33A MnP variants and A48C/A63C/D182C/G214C reflected enzymes that had undergone alkaline transitions and had formed bis(histidyl) heme complexes, whereas the optical spectra of A48C/A63C, which has an additional disulfide bond adjacent to the distal calcium-binding site, was representative of a pentacoordinate, high-spin heme enzyme (Figures 2 and 4). The A48C/A63C mutant MnP was able to prevent the formation of a bis(histidyl) heme complex without exogenous calcium being added to the sample (Figure 3). With the exception of the C33A MnP variants, the addition of calcium (1 mM) to the alkali-treated MnP resulted in the restoration of optical spectra representative of a high-spin state for the enzymes. The addition of exogenous calcium to the alkali-treated C33A variants failed to restore the proteins to an active state. Extreme excess (100 mM) of exogenous calcium was not required to restore alkali-treated enzymes to pentacoordinate, high-spin state.

The effect of exogenous calcium was also considered as a factor influencing A48C/A63C to maintain a pentacoordinate, high-spin state under alkaline conditions. The enzymes had been checked previously for the presence of excess calcium by inductively coupled plasma mass spectroscopy. As we reported earlier (*18*), the average molar ratio of iron to calcium was 1:2, indicating that the purified enzyme did not contain excess calcium that would cause erroneous results in our experiment. The addition of exogenous calcium to alkali-treated A48C/A63C caused a slight increase in the Soret absorption and strengthening of the observed absorption bands indicative of calcium contributing to the structural integrity of the heme environment. We therefore believe that the ability of A48C/A63C to retain the spectral features of a pentacoordinate, high-spin enzyme at alkaline pH is a function of the engineered disulfide bond.

A seventh disulfide bond was introduced into MnP at positions Asp182 and Gly214, analogous to PNP. These surface accessible residues form a disulfide bond ap-

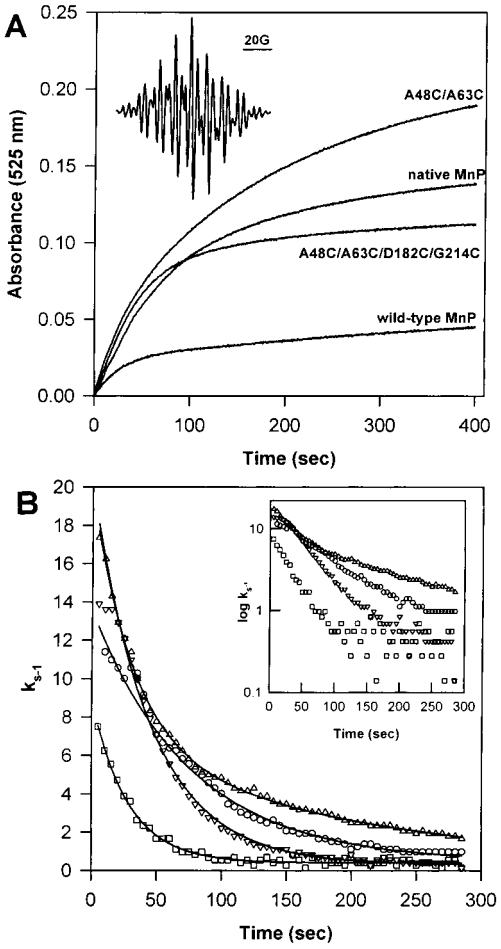

FIGURE 6: Oxidation of Hanker−Yates reagent by MnP at pH 9.0. (A) Kinetic trace of Hanker−Yates reagent oxidation by native MnP, wild-type MnP, A48C/A63C, and A48C/A63C/D182C/G214C. (Inset) ESR spectrum of *p*-phenylenediamine radical obtained during catalytic turnover of MnP. (B) Rate of Hanker−Yates reagent oxidation (measured at five-second intervals) by native MnP (○), wild-type MnP (□), A48C/A63C (△), and A48C/A63C/D182C/G214C (▽). (Inset) Rate data plotted on a logarithmic scale. Experimental conditions are described in Experimental Procedures.

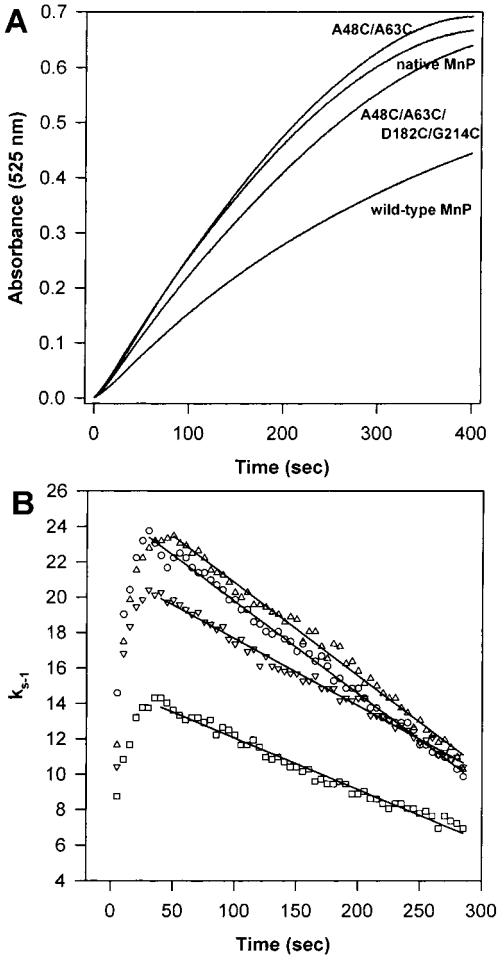

FIGURE 7: Effect of calcium on the oxidation of Hanker−Yates reagent by MnP at pH 9.0. (A) Kinetic trace of Hanker−Yates reagent oxidation by native MnP, wild-type MnP, A48C/A63C, and A48C/A63C/D182C/G214C in the presence of 1 mM calcium ($CaCl_2$). (B) Rate of Hanker-Yates reagent oxidation by native MnP (○), wild-type MnP (□), A48C/A63C (△), and A48C/A63C/D182C/G214C (▽). Experimental conditions are described in Experimental Procedures.

proximately 21 Å from the calcium-binding pocket and bridge the protein strand that extends to and from the proximal calcium-binding site (Figure 1). By analogy to PNP, which retains activity after calcium loss (*25*, *26*), the modification was predicted to enhance the stability of MnP. The inability of A48C/A63C/D182C/G214C to maintain a high-spin heme environment may be the result of the location of the bridging disulfide bond in relation to the path of the protein backbone and the proximal calcium-binding site. The addition of the disulfide bond (D182C−G214C) may have induced conformational changes in the proximal calcium-binding domain, weakening its affinity for calcium, since five of the seven ligands to the proximal calcium are located on this protein segment. The proximal calcium could be lost at alkaline pH, permitting conformational changes that allow movement of the heme and formation of a sixth ligand with the distal histidine (His46).

The thermal and pH stabilities of native MnP, wild-type MnP, and A48C/A63C were reported earlier (*18*). In summary, the addition of a disulfide bond adjacent to the distal calcium-binding site permitted the enzyme to retain greater levels of activity (20%) than native MnP (2%) after exposure to alkaline pH (8.0) at 37 °C. Under similar conditions (pH 8.0, 37 °C, 60 min), the mutant A48C/A63C/D182C/G214C retained nearly 50% activity (Figure 5). At pH 9.0, the enzyme was inactivated to ∼2% activity after a 20 min exposure, a response that was very similar to native enzyme at pH 8.0. The C33A and C33A/A48C/A63C disulfide bond variants exhibited greater instability at pH 4.5 than wild-type MnP (Figure 5).

Because of the low reactivity of MnP with Mn^{2+} at alkaline pH, *p*-phenylenediamine was chosen as the reductant to monitor enzymatic activity at pH 9.0. Oxidation of *p*-phenylenediamine by native MnP, wild-type MnP, A48C/A63C, and A48C/A63C/D182C/G214C illustrated the susceptibility of each enzyme to the effects of pH. Wild-type MnP was most susceptible to inactivation (within ∼75 s) during catalysis at pH 9.0. This rapid inactivation was presumably due to the lack of glycosylation of the protein, which has been shown to have a key role in providing stability to peroxidases (*12*, *27*). In comparison to wild-type MnP, oxidation of *p*-phenylenediamine by glycosylated, native MnP was moderately prolonged (∼200 s), retaining activity for approximately twice the time that wild-type MnP

was active. The A48C/A63C mutant exhibited a faster rate of *p*-phenylenediamine oxidization at pH 9.0 and sustained oxidation for a greater period of time (>300 s) than native MnP. The mutant A48C/A63C/D182C/G214C was also able to oxidize *p*-phenylenediamine at a rate comparable to that of A48C/A63C but the enzyme inactivated within ~150 s at pH 9.0. It is possible that the factors preventing A48C/A63C/D182C/G214C from maintaining a high-spin state (as evidenced by the spectral data) also influenced the abrupt inactivation of the enzyme. Comparison of inactivation rates (t_{0-40} s) for each enzyme showed that the recombinant proteins inactivated at equivalent rates, which were faster than the rate of inactivation for native MnP (Figure 6B). Additionally, the inactivation rates were linear for all enzymes, except A48C/A63C, for which there was a distinct change to a slower inactivation rate at ~50 s (Figure 6B, inset). The similar initial inactivation rates for the recombinant enzymes suggest the lack of glycosylation had a significant effect on their stability. The slower inactivation rate for A48C/A63C may be a manifestation of the ability of this mutant to maintain a pentacoordinate, high-spin heme.

The addition of exogenous calcium to the reactions significantly enhanced the oxidation of *p*-phenylenediamine by MnP, such that each enzyme was able to consume the available hydrogen peroxide within the assay time. Wild-type MnP exhibited a slower rate of oxidation as compared to the other enzymes, perhaps due to the lack of additional stabilizing influences within its structure. The kinetic data show that each enzyme underwent a short period of reactivation during the initial seconds of the reaction. The initial oxidation rates (t_{0-5} s) were similar to the initial rates observed for each enzyme when additional calcium was not present (Figure 6A). The lower activity rates prior to reactivation may be due to structural changes that occur when MnP is exposed to high pH and are reversible when calcium is present. Following addition of calcium, each enzyme exhibited linear rates of inactivation, which may reflect a global effect that pH has on the protein heme environment or structure against which calcium, glycosylation, or disulfide bonds cannot protect.

In conclusion, site-directed mutagenesis was used to introduce multiple disulfide bonds into MnP. These proteins were then evaluated by spectroscopic and kinetic methods to determine the effect of disulfide bonds on the stability and activity of the enzyme. Two disulfide bond combinations were determined to be disruptive of the heme environment and resulted in inactive enzyme. The loss of the disulfide bond at the N-terminus of the B helix was found to increase the sensitivity of MnP to inactivation at high pH, even if a stabilizing, engineered disulfide bond (A48C−A63C) was present in the protein. These data may indicate that the B helix N-terminus disulfide bond is required to maintain active, stable enzyme. The introduction of engineered disulfide bonds into MnP was effective in stabilizing the protein against some of the affects of alkaline pH. A single additional bond in the distal region appeared to be most effective in stabilizing the heme environment and active state of the enzyme. Whereas, the addition of a second engineered bond in the proximal region seem to add a measure of instability back into the protein. The addition of small quantities of exogenous calcium was beneficial to prolong activity of these fungal peroxidases at alkaline pH.

ACKNOWLEDGMENT

We thank Dr. Ming Tien, Penn State University, for his generous contribution of the recombinant MnP expression vector. We thank Cheeyeun Hoor and Deryk Anderson for their excellent technical assistance, Michael Cameron, Guojun Nie, and Sergei Timofeevski for many helpful discussions, and Terri Maughan for secretarial assistance in preparation of the manuscript.

REFERENCES

1. Barr, D. P., and Aust, S. D. (1994) *Environ. Sci. Technol. 28*, 78A−87A.
2. Tien, M., and Kirk, T. K. (1983) *Science 221*, 661−663.
3. Kirk, T. K., and Farrell, R. L. (1987) *Annu. Rev. Microbiol. 41*, 465−505.
4. Dunford, H. B. (1999) *Heme Peroxidases*, Wiley-VCH, New York.
5. Sundaramoorthy, M., Kishi, K., Gold, M. H., and Poulos, T. L. (1994) *J. Biol. Chem. 269*, 32759−32767.
6. Poulos, T. L., Edwards, S. L., Wariishi, H., and Gold, M. H. (1993) *J. Biol. Chem. 268*, 4429−4440.
7. Kindaria, A., Yamazaki, I., and Aust, S. D. (1996) *Biochemistry 35*, 6418−6424.
8. Cui, F., and Dolphin, D. (1990) *Holzforschung 44*, 279−283.
9. Tien, M. (1987) *CRC Crit. Rev. Microbiol. 15*, 141−168.
10. Wariishi, H., Akileswaran, L., and Gold, M. H. (1988) *Biochemistry 27*, 5365−5370.
11. Schuller, D. T., Ban, N., van Huystee, R. B., McPherson, A., and Poulos, T. L. (1996) *Structure 4*, 311−321.
12. Nie, G., Reading, N. S., and Aust, S. D. (1999) *Arch. Biochem. Biophys. 365*, 328−334.
13. Sutherland, G. R. J., and Aust, S. D. (1996) *Arch. Biochem. Biophys. 332*, 128−134.
14. Timofeevski, S., and Aust, S. D. (1997) *Arch. Biochem. Biophys. 342*, 169−175.
15. Sutherland, G. R. J., Zapanta, L. S., Tien, M., and Aust, S. D. (1997) *Biochemistry 36*, 3654−3662.
16. Youngs, H. L., Moënne-Loccoz, P., Loehr, T. M., and Gold, M. H. (2000) *Biochemistry 39*, 9994−10000.
17. George, S. J., Kvaratskhelia, M., Dilworth, M. J., and Thorneley, R. N. F. (1999) *Biochem. J. 344*, 237−244.
18. Reading, N. S., and Aust, S. D. (2000) *Biotechnol. Prog. 16*, 326−333.
19. Nelson, D. P., and Kiesow, L. A. (1972) *Anal. Biochem. 49*, 474−478.
20. Tuisel, H., Sinclair, R., Bumpus, J. A., Ashbaugh, W., Brock, B. J., and Aust, S. D. (1990) *Arch. Biochem. Biophys. 279*, 158−166.
21. Millis, C. D., Cai, D. Y., Stankovich, M. T., and Tien, M. (1989) *Biochemistry 28*, 8484−8489.
22. Kuan, I.-C., Johnson, K. A., and Tien, M. (1993) *J. Biol. Chem. 268*, 20064−20070.
23. Hanker, J. S., Yates, P. E., Metz, C. B., and Rustoni, A. (1977) *Histochem.* 9, 789−792.
24. Piette, L. H., Ludwig, P., and Adams, R. N. (1962) *Anal. Chem. 34*, 916−921.
25. Hu, C., Lee, D., Chibbar, R. N., and van Huystee, R. B. (1987) *Physiol. Plant 70*, 99−102.
26. van Huystee, R. B., Xu, Y., and O'Donnell, J. P. (1992) *Plant Physiol. Biochem. 30*, 293−297.
27. Lige, B., Ma, S., and van Huystee, R. B. (2001) *Arch. Biochem. Biophys. 386*, 17−24.

BI010440I